Hexagonal close-packed Ni nanostructures grown on the (001) surface of MgO

W. Tian, H. P. Sun, and X. Q. Pan[a)]
Department of Materials Science and Engineering, University of Michigan, Ann Arbor, Michigan 48109-1236

J. H. Yu, M. Yeadon, and C. B. Boothroyd
Institute of Materials Research and Engineering, 3 Research Link, Singapore 117602, Singapore

Y. P. Feng
Department of Physics, National University of Singapore, Singapore 119260, Singapore

R. A. Lukaszew
Department of Physics and Astronomy, University of Toledo, Toledo, Ohio 43606

R. Clarke
Department of Physics, University of Michigan, Ann Arbor, Michigan 48109-1120

(Received 2 November 2004; accepted 18 February 2005; published online 23 March 2005)

We report the *in situ* microscopy observation of an unnatural phase of Ni, a highly strained hexagonal close-packed (hcp) form which we believe is stabilized by heteroepitaxial growth on the (001) face of MgO. We find that the nanosized hcp nickel islands transform into the normal face-centered cubic structure when the size of the islands exceeds a critical value (about 2.5 nm thick with a lateral size of ~5 nm). The structural transition proceeds via a martensitic change in the stacking sequence of the close-packed planes. The formation of hcp Ni nanostructures with an unusually large crystallographic c/a ratio (~6% larger than ideal hcp) is very interesting for spintronic and recording applications where large uniaxial anisotropies are desirable. © *2005 American Institute of Physics*. [DOI: 10.1063/1.1890472]

3*d* transition metals exist in three closely related crystallographic phases in nature, namely face-centered cubic (fcc), body-centered cubic (bcc), and hexagonal close-packed (hcp) phase. Due to a small difference in the lattice energies of these crystallographic phases,[1,2] the structures of transition metals can be tuned among these phases by varying the temperature and pressure, or by structural stabilization through heteroepitaxial growth. Ni, Fe, and Co are among the particularly important 3*d* transition metals, because they all show ferromagnetism. Co undergoes a structural phase transformation from hcp to fcc at 425 °C at ambient pressure, while bcc Co that does not occur in nature has been formed by heteroepitaxial growth on GaAs (Ref. 3) and Cr.[4] Fe possesses bcc and fcc structures at ambient pressure, and hcp Fe exists at high pressure. While Ni is fcc at ambient pressure up to its melting point, bcc Ni was also formed by heteroepitaxial growth.[5,6] Although the formation of hcp Ni has previously been reported,[7–9] the nonvacuum synthesis conditions complicate the interpretation of the experimental data, due to the tendency to form hcp Ni_3N and Ni_3C phases in the presence of N and C.

Here we report the observation of hcp Ni which is believed to be stabilized by heteroepitaxial growth on the (001) face of MgO. We have also been able to study, during growth, the evolution of this form of Ni using an *in situ* technique which combines ultra-high-vacuum (UHV) growth and high resolution transmission electron microscopy (TEM). The formation of phase pure Ni was ensured owing to the UHV conditions and the highly purified source material (99.99%) used for the deposition.

Bulk Ni possesses an fcc structure with space group $Fm\bar{3}m$ and lattice constant $a=3.52$ Å at room temperature.[10] MgO also has a cubic structure with the same space group but a different lattice constant $a=4.22$ Å at room temperature.[11] The lattice misfit in the *a*-to-*a* epitaxial alignment, i.e., a cube on cube epitaxial growth, is ~7%.

The simultaneous Ni growth and TEM observations were performed in a modified JEOL-2000V UHV transmission electron microscope designed and dedicated for *in situ* deposition. The growth described in this letter was performed at 120 °C. The deposition rate was ~0.33 Å/min calibrated by *ex situ* Rutherford backscattering spectroscopy. Figures 1(a) and 1(b) show a TEM image and the corresponding selected-area election diffraction pattern (SAED) of Ni islands after the deposition of one monolayer (ML) (bulk equivalent) of Ni. The islands have an average size of

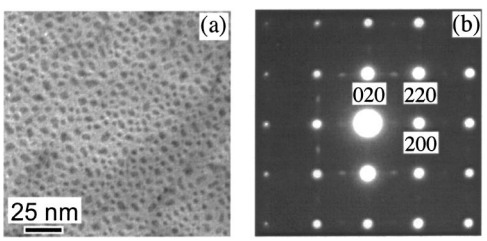

FIG. 1. Transmission electron microscopy (TEM) studies of Ni islands grown on (001) MgO after the deposition of one bulk-equivalent monolayer (ML) of Ni: (a) low-magnification bright-field TEM image of the Ni islands; (b) corresponding selected-area electron diffraction (SAED) pattern. The incident electron beam is along the [001] zone axis of MgO.

[a)]Author to whom correspondence should be addressed; electronic mail: panx@umich.edu

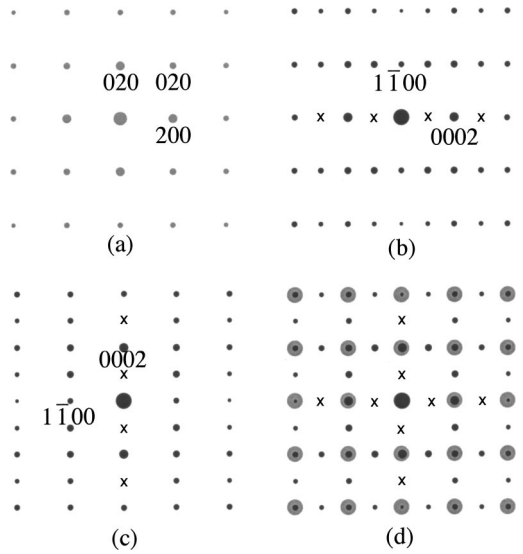

FIG. 2. Computer simulations for the SAED pattern shown in Fig. 1(b): (a) simulation of the [001] zone axis SAED pattern of MgO; (b) simulation of the $[11\bar{2}0]$ zone axis SAED pattern of hcp Ni; (c) simulation of the $[11\bar{2}0]$ zone axis SAED pattern of an orthogonal growth variant, e.g., a 90° rotation counterpart to (b), and (d) superposition of (a), (b), and (c). The crosses mark reflections that are forbidden but appear due to double diffraction. The weak streaking along the [0001] direction of hcp Ni is most likely due to the existence of stacking faults parallel to the (0001) planes.

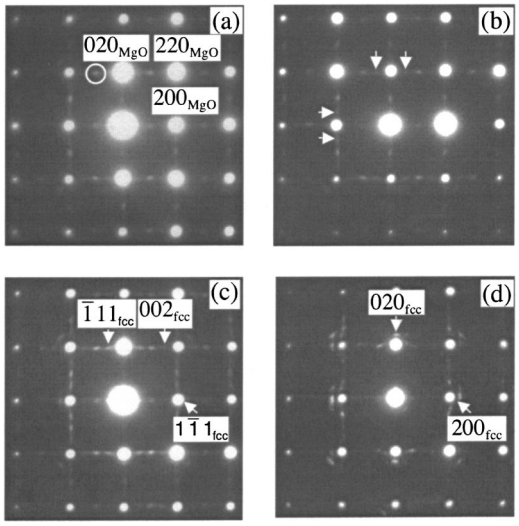

FIG. 3. Selected-area electron diffraction patterns taken during the growth of Ni on MgO from the same area as Fig. 1(a), after the deposition of (a) 1.5, (b) 2, (c) 2.5, and (d) 5 bulk-equivalent monolayers of Ni.

~2.5 nm. The incident electron beam was aligned along the [001] zone axis of MgO and the fundamental diffraction spots of MgO are labeled in Fig. 1(b). No diffraction spots corresponding to the bulk fcc Ni were seen. A striking feature observed is the existence of diffraction spots with weak streaks between the $2h+1\ 2n\ 0$ and $2n\ 2k+1\ 0$ reflections of MgO, where h, k, and n are integers. At the low deposition temperatures of the present work, chemical reaction between Ni and the underlying MgO can be ruled out. Hence, a new structure, which is different from the bulk fcc structure, has to be considered to account for the SAED pattern observed in the nanosized Ni islands.

To determine the structure of the nanosized Ni islands, it is worth revisiting the structures of other members in the 3*d* transition metal family. Bearing the statement in the first paragraph in mind, we speculate that the small Ni islands may have the hcp or bcc structure due to the structural stabilization by epitaxy. Indeed, all the diffraction spots in Fig. 1(b) can be indexed using a hcp structure with lattice constants of $a=2.44$ Å and $c=4.22$ Å. In contrast, the lattice constants of an idealized hcp structure of Ni can be estimated to be $a=2.48$ Å and $c=4.06$ Å, assuming that the interatomic distance remains the same as that in fcc Ni. Figures 2(a) and 2(b) are the simulated [001] zone axis SAED pattern of MgO and the $[11\bar{2}0]$ zone axis pattern of the proposed hcp structure, respectively. Figure 2(c) is also a $[11\bar{2}0]$ pattern of the hcp structure, but with a 90° rotation along the zone axis counterpart to Fig. 2(b). A superposition of Figs. 2(a)–2(c) is shown in Fig. 2(d). One can see that the resulting simulated composite pattern [Fig. 2(d)] reproduces most of the distinct features seen in the measured pattern [Fig. 1(b)]. This suggests that the primary epitaxial orientation relationship between the hcp Ni islands and the underlying MgO substrate is $(11\bar{2}0)<0001>\mathrm{Ni}_{\mathrm{hcp}} \parallel (001)<100>\mathrm{MgO}$. Given the fourfold degenerate characteristics of the (001) surface of MgO, two orthogonal growth variants are expected to occur in the growth plane, namely [0001]Ni ∥ 100]MgO and [0001]Ni ∥ [010]MgO. The lattice constants of hcp Ni are chosen to make the Ni/MgO interface coherent, which is indicated by the SAED pattern. As a result, the hcp Ni islands have a c/a ratio of 1.729, almost 6% larger than the value (1.633) for an ideal hcp structure.

The structural evolution of the Ni islands during growth is revealed by a series of SAED patterns [Figs. 3(a)–3(d)] taken from the same area as shown in Fig. 1(a) after the deposition of 1.5, 2, 2.5, and 5 bulk-equivalent MLs of Ni, respectively. The streaking along the [0001] direction of the hcp Ni is due to the existence of stacking faults parallel to the (0001) planes. The increase in the intensity of streaks in Fig. 3(a) in comparison with Fig. 2(b) indicates the increase of the population of stacking faults in the hcp Ni islands, which we believe is due to the well-known Martensitic transformation from hcp to fcc structure.[12] In Fig. 3(c) new diffraction spots are seen and are caused by the superposition of one [001] and four different [110] zone axis diffraction patterns of fcc Ni. Three diffraction spots indexed in Fig. 3(c) belong to one of the four [110] diffraction patterns, with the orientation relationship of $(001)[1\bar{1}1]$fcc-Ni ∥ (001) [100]MgO. A second [110] diffraction pattern, which has a 90° rotation along the [110] direction with respect to the previous orientation, results from an orthogonal growth variant due to the fourfold degenerate (001) MgO surface. The other two [110] diffraction patterns are caused by the (111) twining of the previous two [110] growth variants. Furthermore, the spots from the [001] oriented fcc Ni structure are also seen in Fig. 3(c) and they are indexed in Fig. 3(d). The orientation relationship between the [001] fcc-Ni and MgO is (001)[100]fcc-Ni ∥ (001)[100]MgO. This result revealed that the hcp Ni nanostructure exists in the early stage of the growth [Figs. 1(b) and 3(a)], followed by the formation of the fcc structure when the islands are thicker than ~2.5 nm. Diffraction spots corresponding to hcp Ni vanished when five bulk-equivalent ML Ni was deposited [Fig. 3(d)]. Thus, the late stage of Ni growth only involves the pure fcc structure. Analysis of diffraction patterns [Figs. 3(b)–3(d)] shows that fcc Ni islands have a lattice constant of 3.54 ± 0.03 Å

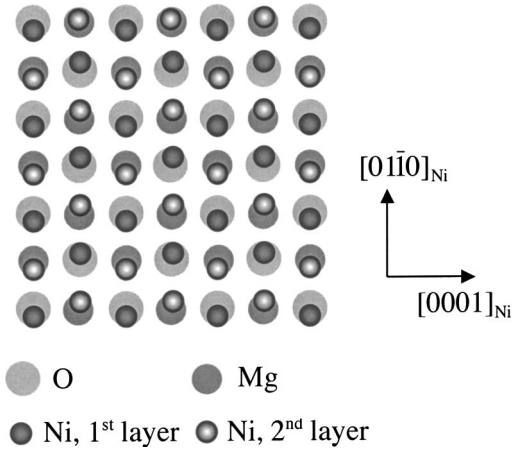

FIG. 4. Diagram showing the arrangement of the first two monolayers of Ni grown on (001) MgO, according to the first principle calculations.

which is within the experimental error to the lattice constant of the bulk fcc-Ni structure (3.52 Å), indicating a relaxed fcc lattice. In contrast, the hcp-Ni/MgO interface consists of coherent strain.

The stabilization of a nonequilibrium hcp Ni phase is believed to be as a result of the pseudomorphic character of the initial growth of Ni on (001) face of MgO. This requires the film to adopt the surface crystal structure of the substrate. To investigate the growth mechanism and to determine the interfacial structure, we carried out a first principles spin-polarized total energy calculation on the MgO (001) surface with 1 and 2 ML Ni coverage, respectively. The supercell used in our calculation consists of a slab of nine MgO layers and two (for 1 ML of Ni) or four (for 2 ML of Ni) Ni layers and a vacuum region of about the same thickness as the slab. Atomic positions in the middle three layers of the slab are fixed to simulate bulk MgO while all atoms in the remaining MgO and Ni layers are fully relaxed. The CASTEP code[13] which is based on the density functional theory[14] and the pseudopotential method was used in our calculation. We used the ultrasoft pseudopotential[15] and the generalized gradient approximation,[16] with a cutoff energy of 340 eV and 9 k points generated according to the Monkhost–Pack scheme.[17] The optimized structure with two Ni monolayers is schematically shown in Fig. 4. The two Ni monolayers have an *abab*…*abab* stacking sequence, namely the hexagonal close-packed stacking sequence, along the <100> direction of (001) MgO. Such a stacking sequence gives rise to a hexagonal close packing of Ni atoms by aligning hcp Ni$[0001] \parallel$ MgO$[100]$ and hcp Ni$[1\bar{1}00] \parallel$ MgO$[010]$, with the Ni atoms displaced slightly from the O^{2-} locations as shown in Fig. 4. The theoretical calculation corroborates the observed hcp Ni structure as well as the epitaxial orientation relationships between hcp Ni and the underlying (001) MgO.

We note that (001) oriented fcc-Ni adopts the surface crystal structure of the substrate as well. Nonetheless, $(11\bar{2}0)$ oriented hcp-Ni is energetically favorable due to its much smaller lattice mismatch with the substrate and a small difference in the lattice energy among the hcp, fcc, and bcc structures in many transition- and noble metals.[1,2,18] The observed epitaxial orientation relationships $[0001]$Ni $\parallel [010]$MgO and $[10\bar{1}0]$Ni $\parallel [100]$MgO correspond to lattice mismatches of 3.9% and 1.8%, respectively, in strong comparison to the ~17% lattice mismatch involved in the cube-on-cube epitaxial growth. Thus, we believe the reduction of misfit strain energy is the driving force that dictates the formation of hcp nanosized Ni islands on (001) MgO.

The transformation from the hcp to fcc structures is believed to emerge at the point when strained hcp Ni nanoislands started to relax. The strain is essentially due to the lattice difference between the ideal hcp Ni structure and the (001) face of MgO. This argument is supported by our TEM observations that fcc Ni possesses a lattice constant close to bulk value from the beginning of its formation. The structure of Ni islands undergoes a hcp to fcc martensitic transformation through the nucleation and gliding of partial dislocations and stacking faults, a process that has been well studied in metals. This transition preserves the close-packed planes and directions in both hcp and fcc structures. As a result, the $[11\bar{2}0]$ axis of the hcp structure becomes the $[1\bar{1}0]$ axis of the fcc structure given that both are close-packed directions. A subsequent reorientation from (110) fcc Ni to (001) fcc Ni was also observed in the late stage of the growth. However, to address this reorientation is beyond the scope of this letter. It will be discussed elsewhere.[19]

Our observations show that the hexagonal close-packed structure, which does not exist in nature for Ni, was stabilized in nanosized Ni crystallites with a lateral size up to 5 nm. Such nanosized hcp Ni subsequently transforms into the normal fcc structure via a martensitic transformation mechanism as the growth proceeds. bcc, fcc, and hcp phases are all found in Co and Fe. Our present studies, together with the previous observations, verified that these three phases can also be realized in Ni.

This work was supported by the National Science Foundation (NSF) through Grant No. NSF/DMR 0308012 (XQP) and by the Institute of Materials Reasearch and Engineering (IMRE) in Singapore.

[1] H. L. Skriver, Phys. Rev. B **31**, 1909 (1985).
[2] A. T. Paxton, M. Methfessel, and H. M. Polatoglou, Phys. Rev. B **41**, 8127 (1990).
[3] G. A. Prinz, Phys. Rev. Lett. **54**, 1051 (1985).
[4] N. Metoki, W. Donner, and H. Zabel, Phys. Rev. B **49**, 17351 (1994).
[5] B. Heinrich, S. T. Purcell, J. R. Dutcher, K. B. Urquhart, J. F. Cochran, and A. S. Arrott, Phys. Rev. B **38**, 12879 (1988).
[6] W. X. Tang, D. Qian, D. Wu, Y. Z. Wu, G. S. Gong, X. F. Jin, S. M. Chen, X. M. Jiang, X. X. Zhang, and Z. Zhang, J. Magn. Magn. Mater. **240**, 404 (2002).
[7] J. G. Wright and J. Goddard, Philos. Mag. **11**, 485 (1965).
[8] S. Illy, O. Tillement, F. Machizaud, J. M. Dubois, F. Massicot, Y. Fort, and J. Ghanbaja, Philos. Mag. A **79**, 1021 (1999).
[9] G. Carturan, G. Cocco, S. Enzo, R. Ganzerla, and M. Lenarda, Mater. Lett. **7**, 47 (1988).
[10] R. W. G. Wyackoff, *Crystal Structure* (Interscience, New York, 1953), Vol. 3.
[11] R. W. G. Wyackoff, *Crystal Structure* (Interscience, New York, 1953), Vol. 1.
[12] G. B. Olson and M. Cohen, Metall. Trans. A **7**, 1897 (1976).
[13] M. C. Payne, M. P. Teter, D. C. Allan, T. A. Arias, and J. D. Joannopoulos, Rev. Mod. Phys. **64**, 1045 (1992).
[14] P. Hohenberg and W. Kohn, Phys. Rev. A **136**, 864 (1964); W. Kohn and L. J. Sham, Phys. Rev. A **140**, 1133 (1965).
[15] D. Vanderbilt, Phys. Rev. B **41**, 7892 (1990).
[16] J. P. Perdew, K. Burke, and M. Ernzerhof, Phys. Rev. Lett. **77**, 3865 (1996).
[17] H. J. Monkhorst and J. D. Pack, Phys. Rev. B **13**, 5188 (1976).
[18] B. I. Min, T. Oguchi, and A. J. Freeman, Phys. Rev. B **33**, 7852 (1986).
[19] H. P. Sun, Y. B. Chen, and X. Q. Pan (unpublished).